Integrated Communications and Energy Management in Intra-body Networks

Anonymous authors

***Abstract*—In this paper, we explore the integrated structure of the intrabody networks, which consist of multiple sensors, a few data aggregators, and decision-makers called the hubs, an On-Body Node (OBN) with more complex capabilities and display features, along with an alternate energy source or backup node in form of a stomach patch. The nodes within the network employ magnetic resonance communication (MRC) technology, which was selected for its favorable propagation properties within biological tissues. Given the limitations of incorporating traditional batteries in implanted devices, these nodes rely on energy harvesting from an external, removable, and rechargeable On-Body Node (OBN), such as a smartwatch. This paper discusses the network architecture that facilitates the degraded mode operation of the network to cope with low battery status and the removal of OBN for charging for longer hours. As we compare a few policies for energy saving mode, we show that proper management of OBN removal can allow for long periods of operation with a small backup node.**

***Index Terms*—Intra-body networks, Magnetic Resonance Communications, Kalman Filtering, Data aggregation.**

I. Introduction

Chronic diseases are becoming increasingly prevalent worldwide, driven by several factors including an aging population in developed nations and escalating levels of pollution—air, water, and food—in developing countries [1], [2]. In the United States, nearly 45% of the population, equating to approximately 133 million people, live with at least one chronic illness [3], and this figure is continually rising. Among U.S. adults, 25% have two or more chronic conditions, while over 50% of older adults (aged 65 and above) are managing three or more chronic conditions [4]. Chronic diseases remain the primary cause of mortality and long-term disability in the country [5].

Recent advancements in medical devices have opened new possibilities for continuous monitoring and automated diagnosis in chronic disease management [6], [7]. In this paper, we explore the structure and features of such networks, which we refer to as Chronic Disease Management Networks (CDMN). A key challenge in these networks is the need for a reliable energy supply and efficient energy use, as batteries are impractical for deeply implanted devices due to their large size as compared with the rest of the electronics and the invasive procedures required for replacement. Thus, integrating energy harvesting mechanisms alongside communication systems becomes crucial. The energy can be harvested internally from dynamic organs like the heart or lungs [8], [9] or can be externally provided by an on-body node (OBN) which we assume to be a smart-watch like device with an antenna to enable both energy transfer and communication with CDMN. However, the focus of this paper is on communications rather than energy distribution per se, which is explored in [10]. However, energy is the most precious resource for CDMN and must dominate all communications related considerations including the media access control (MAC) mechanisms, low-power transition of nodes, and dealing with low-energy scenarios, The paper makes the following key contributions:

1) We devise simple mechanisms to avoid interference between communication, allow configuration of network parameters, support emergency communications, and avoid unnecessary communications via signal prediction.
2) We develop mechanisms to cope with low-energy scenarios, including maximization of operations during these periods, and managing transitions back and forth between different operational modes.
3) We allow for OBN to be removed for charging regularly (e.g., once a day) while still allowing for network continuation and external alerting via a backup node with very long inter-charging time (e.g., a year or more).
4) We evaluate the mechanisms comprehensively via detailed simulations with parameterization covering the characteristics of the body media, energy transfer overheads, communication/computing energy expenditure, etc. We use both centralized and distributed energy transfer mechanisms discussed in [10] in this evaluation.

We show that a 7-node CDMN consisting of 5 sensor nodes and 2 hub nodes can sustain up to 20 hrs/day on energy supplied by a smartwatch like OBN. We also show that if the user forgets to put back the OBN for an entire additional day no more than once a month, the backup can last for a year without risking any shutdown of the operations. **KK:*****Modify this based on the results.

II. Chronic Disease Management Networks

A. Architecture of CDMN

The CDMN can be structured in multiple ways, subject to the constraint of collecting the required signals where they can be tapped inside the body. The sensors are often clustered around the diseased or a crucial body part; thus, we envision CDMN structured as shown in Fig. 1, i.e., a set of ”hub” nodes each interacting with nearby sensors/actuators. Only the hubs interact with the OBN directly. The OBN serves

three primary functions: (a) receiving data from the intrabody network for processing, alerting, and display, (b) transmitting energy to the intrabody nodes as needed, and (c) managing, configuring, and controlling the entire network. The OBN may also interact with external devices through regular networking (e.g., WiFi or BLE), but we do not consider that aspect here. The primary role of a hub is to collect data from its sensor nodes and perform the required data concentration, aggregation, filtering, and processing before sending the results to the OBN. The hub may also manage the configuration of its sensors and control actuation (e.g., drug/electric stimulation delivery). The individual sensor nodes are tasked with receiving energy, gathering data, and transmitting it back to the hub.

With OBN as a regular smartwatch-like device that is likely to be removed for charging or other activities for rather longish periods, we need another wearable device to receive any alerts and for emergency energy supply. Accordingly, we assume a BACKUP node, likely in the form of a stomach patch, that is intended to be used sparingly both for communication and energy supply so that its battery can last for a very long period (e.g., many months or more).

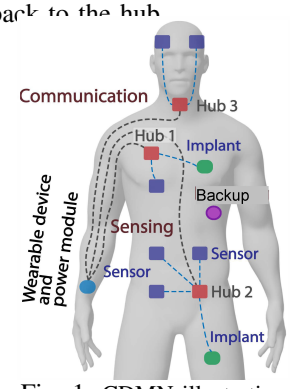

Fig. 1: CDMN illustration

The OBN and backup are assumed to be equipped with a specialized antenna that maintains contact with the skin to enable through-the-body wireless communications (TBWC) and energy transfer. Other CDMN nodes also use TBWC. This requires a suitable Human Body Communications (HBC) technology with very low power, a small antenna, and efficient transmission in the body. We discuss this next.

B. Communications and Energy Transfer Through the Body

It is well known RF is not suitable for HBC [11], [12], but many other technologies have been studied in the literature [13], [14]. Here we focus on Magnetic Resonance Communication (MRC) since it has been demonstrated that it is very well suited for CDMN [15], [16]. MRC uses a resonant pair of transmitter and receiver, each of which has a coil in parallel with a capacitor thereby forming an LC circuit. Such a circuit has a natural resonance frequency given by $1/(2\pi\sqrt{LC})$, traditionally chosen to be 13.56 MHz (RFID frequency), although it was previously discovered that the optimal frequency for intrabody use is around 25-30MHz [17]. The low frequency results in nonradiative energy transfer, primarily through magnetic induction between the two coils. A precise matching of the resonance frequency and impedance on the transmit and receive side results in efficient energy transfer, but the maximum efficiency is limited to 50%. The impedance determines the magnitude of the resonance peak or gain – a higher gain is better but may be more easily perturbed due to various factors including the (human body) channel characteristics, which are affected by physiological parameters. Ref [18] explores an autotuning mechanism to maintain a high gain regardless of perturbations which can be used here.

We have evaluated MRC in an on-body configuration, where both the transmit and receive coils were flat, applied directly to the skin using conductive gel and shielded to minimize through-the-air communication interference. For intrabody applications, MRC coils could adopt alternative geometries but would need to remain small (approximately 1 cm or less in diameter) and enclosed within a biocompatible casing. The details are contained in our energy delivery paper[??]. Attenuation levels for MRC transmission within the body were observed to range between 15 to 23 dB over body-length distances, indicating the feasibility of this technique for intrabody networks. Moreover, the technology exhibited resilience to typical variations expected in both on-body and intrabody environments, including movement, posture changes, clothing differences, and individual physical variations such as body build and weight. Incidentally, simulations using phantom body models show that on-body results closely align with intrabody performance [15]–[17].

C. Coordinating Communications

The most basic issue in any wireless network is the coordination of communications to avoid interference when multiple nodes try to send data to any given node (e.g., from multiple sensors to its hub). In fact, unlike in-the-air networks, communication from any node in the body could potentially be heard by every other node. Furthermore, typically most nodes send a tiny amount of data (e.g., a few bytes to a few tens of bytes) periodically, and the periods tend to be rather large (10's of seconds or more). Given this, a small network, and the need for extreme energy efficiency, we opt for a simple scheduled MAC coordination mechanism, where every node has a set slot to send the data, although the schedule can be changed occasionally as needed through the configuration capability that we consider as an inherent part of the network. An important aspect of a fully scheduled MAC is that the data receiver knows when the data may be transmitted, and it can stay in a low-power mode at all other times.

Fig. 2 shows a sample network with two hubs as a hierarchy. We classify the communications as Keep-Alive (KA) communication and Regular Communication (RC). The RCs concern normal data/energy transfers as required by the application. The KACs have a predefined duration, henceforth called *KA duration* and denoted as Δ^{KA}.

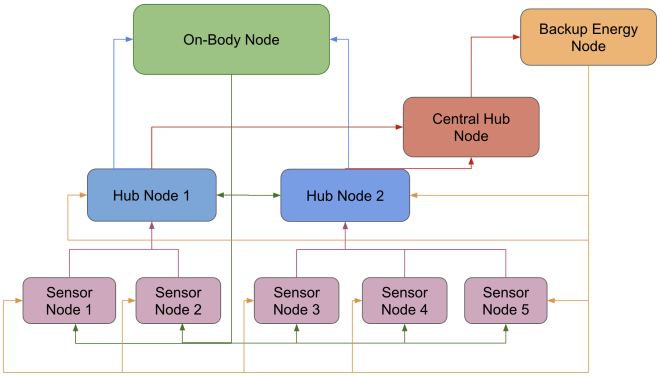

Fig. 2: Diagram of Network Architecture

KK:***Even at full column, the font is so tiny, even though so much space is being wasted on lines and boxes There are two reasons to use KACs. First, they limit the gap between RCs; such a gap may occur either because the node is faulty or because the signal has not changed much, and sending it out is not considered essential (more on this later). Second, they can convey configuration information (as needed) to optimize operational and energy efficiency. In both cases, the KA message conveys the regular data as well (if any). For example, a sensor would typically sense a new value periodically (with duration Δ^{RC} that is a submultiple of Δ^{KA}. If no RC happens for Δ^{KA} duration, the KAC will contain the last sensed value regardless of whether it also conveys configuration information. Because of the asymmetric nature of CDMN, the "keep-alive" aspect of KACs is relevant only in the "up" direction, i.e., from sensor to hub, and hub to OBN, since this is the direction that the data normally travels. For the same reason, the configuration-related KACs go only in the "down" direction, i.e. from OBN to hub, and hub to sensors.

D. Summary of Energy Transfer Techniques

Even though CDMN involves integrate energy transfer and communications, this paper does not focus on energy transfer strategies, which are covered in a different paper [10]. However, for completeness, we mention the strategies here briefly. The energy transfer happens only from OBN, and given a wireless media, some energy will reach every node of CDMN. However, as shown in [10], allowing all the nodes to partake the sent energy is not a good idea since the energy available to any given node goes down as more nodes try to receive it. Accordingly we devised two basic energy transfer mechanisms in [10]: Centralized and Distributed. In the centralized scheme, the OBN decide who should harvest in the next round based on the energy levels and needs of each node, which is communicated to the OBN as a part of KACs. Again, it turns out that allowing everyone who is low on energy to harvest is not a good idea, and instead we set a fixed number K (a hyperparameter of the algorithm). In distributed scheme, each node decides on its own whether to partake the energy based on some thresholds. It turns out that the centralized scheme keeps the nodes better stocked, but only certain values of K work properly. In contrast the distributed scheme is much more robust. We also explore a hybrid scheme in [10] which attempts to enhance both robustness and energy level.

We next discuss a few issues when energy transfer and communications are integrated. There is no conflict between the two: the energy transfer occurs at the resonance frequency (around 25MHz) whereas it suffices to keep the communication occur at a much lower rate (e.g., 250KHz) without introducing too much signal delays. However, there is one subtle issue with integration: a receiver needs to be connected both for energy and signal reception. This means that a receiver who connects to receive only the data will also receive energy during periods of simultaneous transfer. However, this should not have any significant impact since the communication durations are much smaller than energy reception durations.

E. Reducing Communication Energy Expense

Basic communication involves many operations such as packet forming, modulation/demodulation, packet framing, A/D and D/A conversion, signal amplification, error checking, etc. Higher communication layers add to this, and so does wireless transmission, which may result in 20dB or more attenuation. This makes wireless communication quite expensive as compared to computation, especially if the latter is implemented through an ASIC or FPGA. Although the communication energy has been reported for many specific instances (e.g., for RF-based body area networks in [19]), it depends on numerous factors, including significantly on how effectively the protocol and the nodes can make use of low power modes and the packet sizes. With very small packets, as we expect in the CDMN context, the per-byte energy cost of communication can be quite high, which means batching data can provide a useful energy vs. delay tradeoff.

There are many well-known and practiced ways of reducing communication energy, including (a) Continuous signal value prediction using Kalman filter or other means to reduce transmission rate, which provides a tradeoff between signal reconstruction accuracy and energy, (b) Accumulating data before transmission, which provides a tradeoff between delay (latency) and energy, (c) Signal filtering (e.g., subsampling, averaging, thresholding, etc.) that provides a tradeoff between signal fidelity and energy. We shall make use of all these techniques and evaluate the tradeoffs.

The physiological signals may show a variety of behaviors over time, including stable periods, drifts to higher or lower baselines (due to chronic illness, aging, lifestyle factors, etc.), and rapid changes that may last many minutes or longer before returning to normal. It is important to maintain a target accuracy across these different periods. We propose a closed loop control to provide such a capability which can be wrapped around the signal prediction mechanism (at the receiver side) to dynamically adjust signal subsampling or batching on the sender side.

The signal prediction mechanism could range from simple statistical methods to elaborate machine learning techniques,

but only the former is suitable for the hubs. The popular ARIMA (autoregressive integrated moving average) model predicts the next value (or their differences) based on prior values and errors. ARIMA predictions assume stationarity in the samples and do not deal well with missing samples.

In contrast, the popular Kalman filter builds a model of the hidden state of the underlying process, and uses it along with a noise model to predict the measured values. It (a) predicts the (hidden) state at the next time instant based on the assumed system dynamics, and (b) updates the state based on the new measurement received. The Kalman filter does not require stationarity or time-invariance of the parameters and can easily handle missing values by skipping updates. In [20] we have studied such a mechanism in detail which provides an adaptive closed-loop control over the transmission. The data sender defines a threshold $\epsilon \in [0, 1]$ as a tolerance such that the prepared sample (individual or batch) will be transmitted only if the fractional difference between it and the previous value exceeds ϵ. The receiver continues predicting next sample until it receives one when it computes the error estimate which is checked against some error threshold κ. If the error exceeds κ, the receiver estimates a new value of the threshold ϵ and sends it as feedback to the data sender. The goal is to make ϵ as large as possible (to reduce communications) and yet keep the signal reconstruction error at the hub within specified bounds. It is shown in [20] that the mechanism can significantly reduce the number of communications and we shall employ it for every periodic signal transfer.

III. Energy Efficient Communications in CDMN

A. Time-Slot Allocations

We consider a common global clock tick for all the nodes for communication scheduling. We consider δ as the tick duration, which represents the sampling rate of the fastest signal inside the body (usually 100ms or more). We will define longer time slots as integer multiples of δ. In particular, $\Delta^{RC}(j) = k_j^{RC}$ is the minimum duration for regular communications for node j, where k_j^{RC} is an integer. Similarly, $\Delta^{KA}(j) = k_j^{KA} \times \Delta^{RC}(j)$ is the duration for sending the keep-alive message by node j, where k_j^{KA} is also an integer, typically the same for all nodes under a hub.

In the CDMN environment, all communications are expected to be rather short. In particular, a single sample from even a sensor that can sense multiple parameters will likely be $\sim$10 bytes, and batching them will result in at most a few hundred bytes. At $\sim$25 MHz resonance frequency, MRC can easily support 1 Mb/sec with simple BPSK modulation, and thus the total packet forming and transmission time can be kept under 1 ms, which would be much smaller than δ. The sample collection itself could be quite slow (e.g., blood glucose measurement) but this does not matter for transmission scheduling. We assume for convenience that an entire δ slot is used for communication. Given the rather small size of the network, most delta slots will remain unoccupied and can be used for sporadic or emergency communications. Fig. **??** shows the size difference of different time slots.

B. CDMN Application Types

The CDMN discussed here may be used to support a wide variety of intra-network applications, that differ not only in terms of network size/configuration (e.g., the number of hubs & sensors connected to them) but also in terms of how data is collected, transmitted, and processed. Because people increasingly suffering from multiple chronic diseases, the CDMN will likely support multiple applications *simultaneously*, each using a subset of nodes, with some sensors and hubs involved in multiple applications. If a sensor supplies the same data to the same hub for two different applications, the more stringent requirements will prevail. In addition to therapeutic applications, one could also define some "utility" applications that periodically collect and display statistics regarding both the data and health/configuration for all the nodes. In the following, we consider some important variations.

The data transmission needs of various applications can vary substantially but can be divided into two broad classes. In a streaming application (SA), the hub generates another time-series by processing the incoming streams from its sensors and sending it to the OBN. Since various sensors may have different time-periods, the hub may need a batch of data from each of its sensors before processing and sending the output to the OBN. In a non-streaming application (NA), the hub only sends sporadic alerts or statuses to the OBN. For both application types, the hub would use a Kalman filter to reduce the transmissions from the sensors, but a Kalman filter at the OBN is sensible only for SAs.

By default, a sensor sends one value per sensing period and a classical Kalman Filter is adequate to handle it. However, given the very small size of the transmissions, it is more efficient for a sensor to accumulate a batch of sensed values and then send to the hub. In this case, we need to extend the Kalman filter to vector data, Such clustered transmission (CT) essentially trades off energy for latency, which may be acceptable for fast signals. In CT, the sensor retains the previous data vector $v^{(prev)}$ as well. When the current vector $v^{(curr)}$ is complete, it computes the RMS value of the difference, i.e., $\sqrt{(\sum_{k=1}^{K}(v_k^{(curr)} - v_k^{(prev)})^2/K)}$ and compares it against the threshold to decide if $v^{(curr)}$ should be transmitted. In case of transmission, we let $v^{(prev)} = v^{(curr)}$. On the hub side, the Kalman filter now needs to predict the entire vector, and when the next vector is received, it uses the RMS value of the difference between the predicted and received vectors to estimate the error. We will study the Kalman filter performance as a function of the batch-size for CT.

IV. Experimental Design

For our evaluation, we use a three-hub network, where Hub 1 manages sensors 1-2 and Hub 2 manages sensors 3-5, with a backup node integrated to ensure redundancy and operational

continuity. *The third Hub Node is considered the central hub node*, which establishes communications with both the hub nodes as well as the backup energy node. The *central-hub* node acts as an intermediary between the hubs and the backup energy node in the absence of the OBN. This design was selected for its ability to balance communication efficiency, load distribution, and error tolerance while maintaining manageable system complexity. The central-hub receives data and energy levels from the hubs when the OBN is removed from the network for some time. Then the central-hub communicates with the backup energy node by sending a wake-up call to the backup energy node. The Backup wakes up and, based on the central-hub's decision, it employs one of the energy transfer strategies - Centralized, Decentralized, and Hybrid, to provide energy to the nodes that are in the low energy mode, and performs energy transmission to them. However, the backup energy node can only achieve that twice before returning to the sleep mode again. Therefore, the current central-hub model offers an optimal trade-off, balancing efficient data flow, fault resilience, and reliability for the intended application.

The simulation environment is created using Python. The characteristics of the transmission media (i.e., the human body) were obtained by conducting real on-body experiments. The energy consumption was estimated by using data sheets of available products where possible (e.g., supercapacitors, microcontrollers) and by analyzing the approximate number of instructions to perform various operations. We assume six sensors strategically placed on various parts of the human body, tasked with monitoring key physiological parameters and driven by data traces as described below.

A. Pre-processing of Datasets Used

HK: We also talked about the data here

Table I shows the notations used in the paper.

TABLE I: Notation

Variable	Definition
δ	Basic slot (unit of time discretization)
$\Delta^S(j)$	Sampling and Filtering period of component j (an integer multiple of Δ)
$\Delta^{RC}(j)$	Regular Communication (RC) Communication period of component j
$\Delta^{KA}(j)$	Keep Alive (KA) Communication period of component j (an integer multiple of $\Delta^{RC}(j)$).[1]
k_j^S	Ratio of $\Delta^S(j)$ to δ
k_j^C	Batch size (Ratio of $\Delta^{RC}(j)$ to $\Delta^S(j)$)
k_j^K	Ratio of $\Delta^{KA}(j)$ to $\Delta^{RC}(j)$
N	Total number of nodes
ϵ	Data Threshold

B. Network Scheduling

Following the preparation of the datasets through appropriate subsampling and configuration for signal transmission to the hub nodes, the focus shifted to network scheduling. A structured scheduling mechanism was implemented to allocate dedicated transmission slots for each node, ensuring conflict-free communication across the network. To achieve this, the **Greedy Perturbation Algorithm** was employed, which ensures periodic, non-overlapping transmissions among network nodes. The algorithm calculates the *Least Common Multiple (LCM)* of the nodes' operational periods to define a unified scheduling frame, facilitating synchronized periodic data exchange. Transmission times are derived based on the individual periods of each node and constrained within a predefined time window. Potential conflicts between node transmissions are iteratively resolved through a greedy strategy, applying incremental shifts of 100 milliseconds to overlapping slots until all conflicts are eliminated. These adjustments are tracked to maintain conflict-free scheduling across all nodes while preserving the periodicity of data transmission.

TABLE II: Scheduling for Sensor Nodes

Nodes	Sampling period Δ^S (s)	Reg. comm. period Δ^{RC} (s)	Keep-alive period Δ^{KA} (s)
Sensors 1,2,3,4	2	30	300
Sensor 5	300	300	-

TABLE III: Scheduling for Hub Nodes

Nodes	Down comm. period Δ^F (s)	Up comm. period Δ^{RC} (s)	Keep-alive period Δ^{KA} (s)
Hub 1	120	240	2400
Hub 2	120	420	4200

Tables II and III provide the scheduling parameters utilized for the sensor and hub nodes respectively. The Down comm period Δ^F, determines the frequency of feedback signals transmitted by the hubs to their respective sensors, making threshold adjustments invoked by Algorithm **??**. The Up comm period Δ^{RC} is the sensor equivalent for regular communication frequency.

The sampling and filtering period, denoted as Δ^S, is uniformly set to 2 seconds for all sensors except Sensor 5, which operates with a native sampling period of 300 seconds. The *Regular Communication Period*, Δ^R, defines the interval between consecutive data transmissions and is set to 30 seconds for Sensors 1 through 4, while Sensor 5, aligned with its native sampling rate, uses $\Delta^R = 300$ seconds. Sensor 1 transmits periodically without perturbation, while Sensors 2 through 4 apply the Greedy Perturbation Algorithm to avoid simultaneous transmissions, introducing incremental shifts of 100 milliseconds between nodes.

The *Keep-Alive Period*, Δ^K, is the time interval at which a sensor transmits a signal if it misses ten consecutive regular communication periods (Δ^R), so the number of mandatory communications could only be 10% of the total possible regular communications per hour. This mechanism prevents prolonged communication gaps and ensures network connectivity. Δ^K is set to ten times Δ^R, resulting in 300 seconds for Sensors 1 through 4, and since Sensor 5 employs direct transmission mode, it does not require a KA signal. While Δ^K primarily serves as a fallback for extended inactivity, it mirrors the behavior of regular transmissions at a reduced frequency to conserve energy.

The hub nodes follow a similar structured schedule. The *Threshold Feedback Signal Period*, Δ^F, determines the frequency of feedback signals transmitted by the hubs to their respective sensors, aiding in threshold adjustments for data transmission control. Both hub nodes transmit feedback after receiving four consecutive regular communications, setting Δ^T to 120 seconds. Additionally, the *Hub Communication Period*, Δ^H, regulates the frequency of data aggregation and transmission from the hubs to the OBN. Hub 1 transmits data to the OBN every 240 seconds after collecting information from its associated sensors, while Hub 2 transmits every 420 seconds, aligning with the 300-second regular communication period of Sensor 5. The central-hub utilizes either Hub 1 or Hub 2 timeslot to communicate with the Backup Energy Node when the OBN is absent.

The OBN operates on a standardized communication interval of 600 seconds, ensuring synchronization across the entire network. This duration accounts for the OBN's dual role as both the primary energy source and the controller for configuration updates while maintaining efficient data flow and avoiding transmission congestion.

C. Energy Management Architecture

In this section, we discuss the management of low-energy scenarios caused by low-charge or absence of the OBN. The OBN is designed for daily removal for charging purposes without having to curtail the CDMN operation; however, the CDMN still needs to be able to post any important health alert externally during OBN's removal. As already discussed, this is provided by the Backup node, which can also emergency energy infusion in CDMN to cover situations where the patient fails to put back the OBN within the maximum designed off period. Backup itself is intended to be worn all the time[2] and powered by a non-rechargeable and long-lasting battery. To support this we introduce four energy states for CDMN operation:

HE: This is a high-energy state where the node operates at full capacity with normal sampling rates and communication periods.

LE: This is a low-energy state where the node communicates only at Keep-Alive (KA) interval, skipping regular communication slots.

LE-I: This is a transient state where the node is in low energy mode but still inoperational. It is needed as explained below.

ZE: This is a zero-energy state where the node shuts down and goes into a low-power mode (if any). Only the energy reception circuit is active and will activate the rest of the node when the energy level crosses some threshold.

Normally, the OBN will provide energy periodically to all internal nodes, and its absence (whether from energy depletion or removal) triggers the backup system. A backup node takes responsibility for network energy provision during OBN's absence. The energy distribution system is designed to maintain minimum required energy levels as far as possible. If the energy supply stops, nodes transition to progressively lower energy states until some node reaches ZE. This node notifies its hub in one last communication before it shuts down (goes to ZE). The hub could then take appropriate action.

Since different nodes may reach the ZE at different times, the network should ideally handle loss/addition of a node anytime. However, this would require hubs and indeed the entire network to have the capability to reconfigure – both physically and operationally to cope with changing number of signal streams, and might even be unsafe for correct actuation. Given the energy poor environment, we instead strive to maximize the uptime of the entire network. Thus if any sensor moves into ZE, we simply shutdown the entire cluster operation since the other nodes are likely to be close to the shutdown level already. However, the hub itself remains up as long as possible.

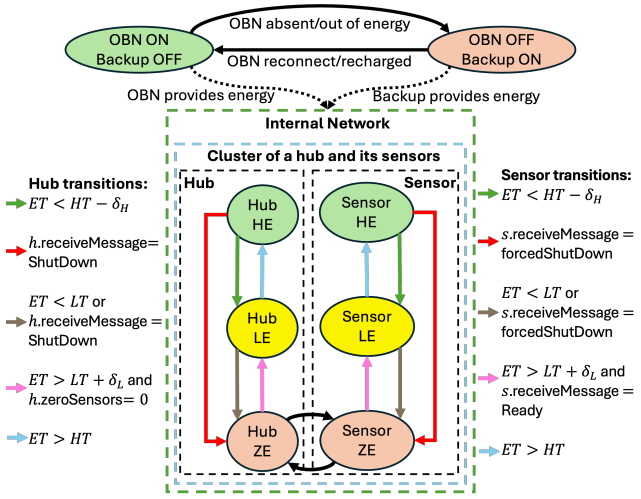

Fig. 3: Network State Diagram

The down transition into a state and up transition from that state must have hysteresis to avoid ping-ponging. We achieve this by introducing 4 parameters: (1) HE threshold (HT), (2) ZE threshold (ZT), (3) HT margin δ_H, and (4) ZT margin δ_L. Transition to LE occurs if the energy level falls below $HT - \delta_H$, and upshift occurs when the energy level exceeds H. A downshift to ZE occurs when the energy level goes below ZT, and an upshift to LE occurs when it crosses $ZT + \delta_L$. Fig 3 shows the state diagram of the network operations.

If the entire network or some of its clusters shut down, the recovery requires a systematic approach as follows:

1) When the OBN returns it provides energy to all nodes in ZE state **KK:*****Is this correct?, and waits until a hub responds.[3] If the hub is in LE/HE, it will respond immediately and otherwise it will respond when it transitions to LE-I state.

[2]Note that it is possible to remove Backup or change its battery while OBN is on.

[3]A shutdown allowed to happen by Backup (while OBN is off) will not be reversed since Backup needs to conserve its energy.

2) If (or when) a hub is awake, it sends a "wake-up" message to all its sensors. The sensor will respond immediately if in LE/HE, and otherwise when it transitions to LE-I. (If the sensor wakes up before its hub does, it will stay in LE-I state w/o sending any data/message to its hub). **KK:*****I took out "central-hub" here – not needed
3) Once a hub knows that all its sensors are awake, it transitions to LE state and sends a message to its sensors to do the same. Normal functioning then resumes.

The state diagram of cluster recovery is shown in Fig 4, where the transitions between each pair of states are depicted.

V. Back-up Policies

Backup can use Centralized or Decentralized strategies, based on its capabilities. However, although OBN and backup both provide the energy and the set up may seem the same, there are inherent differences between the two: OBN provides energy on a schedule. Backup on the other hand, has to choose the best moment and the best set of receivers to delay the network shutdown. For this reason we define the survival time of each node i as the time it has until reaching the shutdown. At time of OBN disconnection T':

$$\int_{T'}^{T'+T_i} e_L(t)dt = E_i(T') - ZT_i \tag{1}$$

Where e_L is the actual consumption of the node. To approximate the survival time (with a fixed time constant, e.g. an hour), we can use:

$$\hat{T}_i = \frac{E_i(T') - ZT_i}{C(\hat{\mu}_i + \hat{\sigma}_i) + R_i} \tag{2}$$

Where $E_i(T')$ is the current energy of node i at time t, ZT_i is the zero threshold, C is the transmission cost and R is the cost of the rest of the operations (all in %). The values $\hat{\mu}$ and $\hat{\sigma}$ are the mean and standard deviation of communications in the time constant (reception and transmission), which can be incrementally updated. It is also possible to use the same ARIMA model to predict the number of communications and (requires passing on the values of the model). Backup uses Modified Centralized strategy that changes the number of receivers: calculate the minimum residual time (survival time of the lowest node could suffice), iterate from 1 to a fraction of the maximum number of selectable receivers, for each iteration, calculate the new survival time and the objective would be $\max \min_i T_i$.

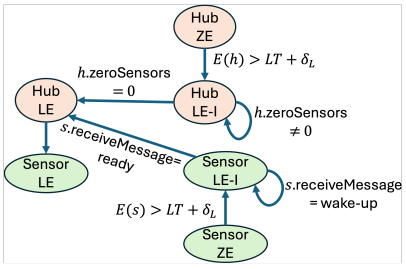

Fig. 4: Cluster Recovery

HK: Fault detection mechanism

VI. Experimental Results & Discussion

A. Simulation Environment

We consider the same proposed simulation environment from our previous work [10], each implantable sensor node is modeled with a 0.5 F CAP-X supercapacitor (model GY12R705012V504R [21]) operating at 3 V, which provides a total energy storage capacity of approximately 2.25 J. The leakage energy cost is determined by considering a quiescent leakage current of 1 μA, leading to a leakage power of 3 μW, and over a specified duration, the total energy loss amounts to 0.0009 J or 0.00025 mWh. The cost associated with Equivalent Series Resistance (ESR) is computed using an average current draw of 2.5 mA and a DC ESR value of 570 mΩ, resulting in a resistive power loss of 3.5625 μW and a total energy loss of approximately 0.00107 J or 0.00030 mWh. For rectification, we assume an ultrasonic-powered rectifier similar to the one proposed by Laursen, with energy consumption comparable to the dual-path RF CMOS rectifier reported by Lu et al. (2017), incurring an energy overhead of approximately 2 mJ or 0.00056 mWh. As the modulation unit for intrabody communication, we adopt the TI CC1101 RF transceiver, a widely used ultra-low-power component for physiological signal telemetry in wireless sensor networks[4]. According to the datasheet, the device draws a typical transmit current of 14 mA, and the energy required for one transmission event is estimated at 171.9 μJ, equivalent to 0.00004778 mWh. For demodulation, we consider a fully digital 28 nm Bulk CMOS BPSK demodulator, as proposed in recent biomedical communication research, which exhibits extremely low power characteristics, consuming approximately 645.12 pJ or 1.791×10^{-10} mWh per operation[5]. **HK:** Is it a battery or a supercapacitor? If it is a supercapacitor, add the reference to its datasheet - **PP:** Referred to the supercapacitor datasheet.

In the subsequent stage of our simulation, each implantable hub node is modeled with a 0.8 F CAP-X supercapacitor (GY12R76C012V804R) operating at 3 V, yielding a total energy capacity of 3.6 J. The leakage energy cost is derived from a quiescent current of 2 μA, resulting in a power loss of 6 μW. Over a time window of 300 seconds, the corresponding energy loss is 0.0018 J or 0.0005 mWh. The energy loss attributed to Equivalent Series Resistance (ESR) is calculated using an average current of 4 mA and a DC ESR of 440 mΩ, leading to a resistive power dissipation of 7.04 μW, and an overall energy loss of approximately 0.00002112 J or 0.00147 mWh. For the rectification process, we assume the use of an ultrasound-based rectifier analogous to the dual-path RF CMOS design proposed by Lu et al. (2017), with a corresponding energy consumption of 2 mJ or 0.00056 mWh. The modulation subsystem for intrabody wireless communication is based on the TI CC1101 RF transceiver, which is well-suited for ultra-low-power applications such as physiological signal telemetry in body sensor

[4]https://www.ti.com/lit/ds/symlink/cc1101.pdf
[5]https://www.researchgate.net/publication/358842273_A_28_nm_Bulk_CMOS_Fully_Digital_BPSK_Demodulator_for_US-Powered_IMDs_Downlink_Communications

networks[6]. According to its datasheet, the device consumes a transmit current of 14 mA, and the energy expenditure per transmission is estimated to be 171.9 μJ or 0.00004778 mWh. The demodulator is modeled using a 28 nm Bulk CMOS digital BPSK demodulation architecture, with an energy cost of 645.12 pJ per reception, equivalent to 1.791×10^{-10} mWh[7].

The OBN is modeled similarly to the Apple Watch Ultra 2 in terms of energy capacity and physical constraints. Although precise component-level energy breakdowns for the Ultra 2 are not publicly available, we estimate power characteristics based on prior Apple Watch models and comparable smartwatches. The modulator is assumed to consume approximately 1–2 mWh per hour, while the rectifier and demodulator contributions are not explicitly documented but are considered negligible under low-power operation. The Apple Watch Ultra 2 features a 564 mAh lithium-ion battery and provides up to 36 hours of usage under typical conditions, with minimal Bluetooth usage. Additionally, an external backup node (e.g., stomach patch) is modeled as a skin-mounted device equipped with a 1000 mAh power bank, offering 3000 mWh of energy. Currently, there are no publicly documented wearable patches for physiological signal monitoring that utilize a 1000 mAh battery, as most designs prioritize compactness and patient comfort by employing significantly smaller energy storage solutions. For instance, a study published in *Science Advances* describes an at-home wireless sleep monitoring patch powered by a 150 mAh lithium-polymer battery, achieving a battery life of approximately 10.55 hours while maintaining wearability and functional integrity[8]. However, to meet our long-term operational objective of achieving a battery life of at least one year, we adopt a wearable research patch architecture supplemented with an external power bank, as demonstrated in flexible sensorized garment designs discussed in recent literature[9]. We consider a 1000 mAh external Li-ion power bank operating at 3 V, with component-wise energy usage estimated over 10 hours.

We assume a signal attenuation of approximately 19 dB per transmission link for a single node. For each additional node added to the network, an incremental path loss of approximately 1 dB is considered. As a result of this significant attenuation, it is estimated that approximately 98.4% of the transmitted energy is lost before reception.

The computational and communication energy costs for each node are based on metrics used in prior literature on energy-aware intrabody networks. The energy metrics for transmission from the OBN and backup node are outlined as follows:

Energy Cost per Action

Each node in the network performs a set of fundamental operations such as data transmission, reception, sensing, and Kalman Filter-based prediction (Only applicable to Hub Nodes) . These actions contribute to the total energy consumption and are essential for understanding the energy profile of the system. The table below summarizes the energy expenditure associated with each of these actions, calculated based on power and duration values. This information is vital for optimizing energy efficiency in low-power sensor networks.

Action	Energy consumed(nJ)	Duration (ms)
Transmission		5
Reception		5
Sensing	200	200
KF (Predict)	90	1.2
KF (Predict + Update)	180	2.4

TABLE IV: Energy Cost per Action for Sensor and Hub Nodes

Energy Costs per component:

- **28 nm CMOS Demodulator:** 645.12 picojoules or 1.791×10^{-10} mWh
- **28 nm CMOS Modulator (Approx value as data not available):** 645.12 picojoules or 1.791×10^{-10} mWh
- **Rectifier Loss:** For sensors and hubs, approx 10% of the total received power from OBN and Backup. For OBN, the rectifier cost is considered within the 3.13% of the natural battery drainage.

Leakage Cost:

- For the **sensors**, the leakage power is calculated as: $P = 3\,\text{V} \times 1\,\mu\text{A} = 3\,\mu\text{W}$. Over a duration of 30 seconds, the energy loss is: $E = P \times t = 3 \times 10^{-6} \times 30 = 9 \times 10^{-5}\,\text{J} = 2.5 \times 10^{-5}\,\text{mWh}$.
- For the **hubs**, the leakage power is: $P = 3\,\text{V} \times 2\,\mu\text{A} = 6\,\mu\text{W}$. Over 30 seconds, the energy loss is: $E = 6 \times 10^{-6} \times 30 = 1.8 \times 10^{-4}\,\text{J} = 5.0 \times 10^{-5}\,\text{mWh}$.
- For the **OBN**, the leakage cost is accounted for within the approximate 3.13% natural battery drainage rate and is not separately computed.

Signal Attenuation: For 1 receiver, average path loss is estimated around 18 dB, and with roughly a 1 dB loss for each additional node added.

The following table lists the energy cost of MCU operations in **active mode** for each sensor node action. The energy values are computed assuming an operating voltage of 3V and an active current of 67 μA. Each action draws energy for the specified duration and is calculated individually.

Convert to Joules

Action	MCU Energy Cost (J)
Transmission	2.79×10^{-8}
Reception	2.79×10^{-8}
Sensing	1.12×10^{-6}
KF (Predict)	6.70×10^{-9}
KF (Predict + Update)	1.34×10^{-8}

TABLE V: MCU Energy Consumption in Active Mode (3V, 67 μA)

[6]https://www.ti.com/lit/ds/symlink/cc1101.pdf

[7]https://www.researchgate.net/publication/358842273_A_28_nm_Bulk_CMOS_Fully_Digital_BPSK_Demodulator_for_US-Powered_IMDs_Downlink_Communications

[8]https://www.science.org/doi/10.1126/sciadv.adg9671

[9]https://www.mdpi.com/1424-8220/21/3/814

In **sleep mode**, the MCU draws only $1.39\,\mu$A at 3V. This corresponds to a power consumption of 4.17×10^{-6} W. For a duration of 1 second, the energy cost in sleep mode is 1.158×10^{-6} mWh.

HK: 1.266ms for prediction; 2.452ms for prediction+update 0.4 nano joules per instruction 33 67 micro ampere 1.39 micro ampere 10 micro s wake up from EM2 How much it takes to transmit 1 byte vs executing 1 instruction

1 byte preamble 1 byte protocol 2 byte CRC 1 byte for receive id 1 byte for transmit id

16 bytes per packet, 8 instructions/byte=128 instructions

872 instructions total, 104+768

128 instructions+104 overhead=232, However we need to even increase this one to include a bunch more

B. Low Energy Scenario in one sensor with OBN present

In this experimental configuration, the OBN, modeled as a smartwatch, is designed to transmit energy to all sensor nodes within the system wirelessly. The OBN delivers energy every 300 seconds, amounting to a total transmission of $4.7268\,$J per hour, equivalent to $0.375143\,$mWh. For each individual sensor node, this corresponds to an energy delivery of $0.0053510519220\,$mWh. However, due to the substantial signal attenuation modeled as a $19\,$dB path loss (2 receivers are connected, the effective energy received by each node is drastically reduced. After accounting for this attenuation, the energy received by a node is approximately $0.003743\,$mWh per transmission, indicating an energy loss of about 98.41% during wireless transmission.

C. Low Energy Scenario in one sensor with OBN absent, Back Up Node is Utilized

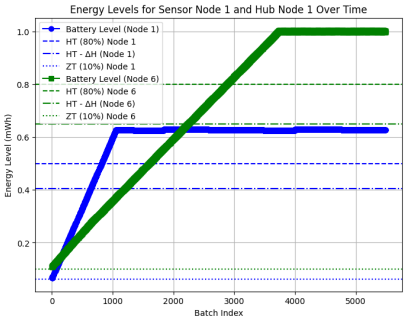

Fig. 5: Sensor 1 - Low energy Mode Recovery (BkUp Present)

The backup node, represented as a skin patch with an external power source, retains a total energy reserve of $150\,$mWh, accounting for 2% of its full $3000\,$mWh capacity. Similar to the OBN, it experiences a $19\,$dB signal attenuation, resulting in a received energy of approximately $1.077442\,$mWh per transmission at the sensor node. Despite these losses, the backup node is configured to supply energy to each node a maximum of two times during critical LE states.

Experimental validation confirms that a single recharge from the backup node is generally sufficient to elevate a node's energy level from zero to its maximum battery capacity.

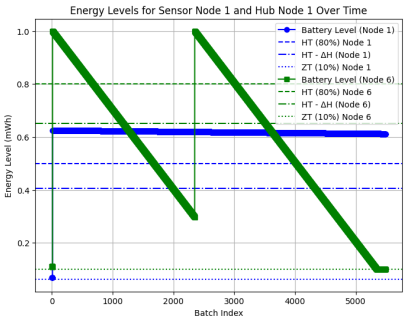

HK: You over-explain the obvious and under-explain the results: there is a page and a half on the energy consumption. Also the components have not change. Did you do the simulations with the old components? have you find the right components? The simulations are very vague as you did not mention what each one is: Why does it seem like there is a smooth upward/downward energy trajectory? doesn't the total 1 hour loss of the nodes change? If yes, then why does it look like a line with positive/negative slope in the figures? The behavior of the hubs also look suspicious: Why does it seem like the hubs are consuming very much larger amount of energy?

D. Sensor and hub operations in a low-energy network

VII. Conclusions

In this paper, we explored an architecture for batteryless intra-body networks to manage chronic illnesses and examined the key issue of highly energy-limited operations. In particular, we explored the trade-off between communication accuracy and energy efficiency via a closed-loop Kalman filter-based prediction of the signals. It is seen that in most cases, it is possible to reduce communications while maintaining a high level of accuracy significantly. Since communications are generally quite expensive, the technique can achieve considerable energy savings as well. We also explored the operation in low energy availability scenarios where we attempt to keep the network operational as long as possible by switching to the degraded mode of operation when the energy-supplying wearable node has been removed for long periods. In the future, we will explore dynamic tuning of various parameters in order to adjust them automatically without any manual intervention.

References

[1] W. H. Organization, "World report on aging," https://iris.who.int/bitstream/handle/10665/186463/9789240694811_eng.pdf, 2015.

[2] G. Yang, L. Xie, M. Mäntysalo, X. Zhou, Z. Pang, L. Da Xu, S. Kao-Walter, Q. Chen, and L.-R. Zheng, "A health-iot platform based on the integration of intelligent packaging, unobtrusive bio-sensor, and intelligent medicine box," *IEEE transactions on industrial informatics*, vol. 10, no. 4, pp. 2180–2191, 2014.

[3] L. P. Fried, "America's health and health care depend on preventing chronic disease," https://www.huffingtonpost.com/entry/americas-health-and-healthcare-depends-on-preventing_us_58c0649de4b070e55af9eade, March 2017.

[4] A. Tinker, "How to improve patient outcomes for chronic diseases and comorbidities," http://www.healthcatalyst.com/wp-content/uploads/2014/04/How-to-Improve-Patient-Outcomes.pdf, 2017.

[5] M. Comlossy, "Chronic disease prevention and management," in *National Conference of State Legislatures*, 2013, pp. 1–16.

[6] H. Y. Tung, K. F. Tsang, H. C. Tung, K. T. Chui, and H. R. Chi, "The design of dual radio zigbee homecare gateway for remote patient monitoring," *IEEE Transactions on Consumer Electronics*, vol. 59, no. 4, pp. 756–764, 2013.

[7] H. Tung, K. Tsang, K. Lam, B. Li, L. Yeung, K. Ko, W. Lau, and V. Rakocevic, "A mobility enabled inpatient monitoring system using a zigbee medical sensor network," *Sensors*, vol. 14, no. 2, pp. 2397–2416, 2014.

[8] C. Saha, T. O'Donnell, N. Wang, and P. McCloskey, "Electromagnetic generator for harvesting energy from human motion," *Sensors and Actuators A: Physical*, vol. 147, no. 1, pp. 248–253, Sep. 2008. [Online]. Available: https://linkinghub.elsevier.com/retrieve/pii/S0924424708001398

[9] K. Li, Q. He, J. Wang, Z. Zhou, and X. Li, "Wearable energy harvesters generating electricity from low-frequency human limb movement," *Microsystems & nanoengineering*, vol. 4, no. 1, pp. 1–13, 2018.

[10] H. Kia, P. Pandit, and K. Kant, "Energy transfer strategies in magnetic resonance based intrabody networks," *Proc. WoWMoM conf., Available at https://www.kkant.net/Hirsa_CDMN_energy_paper.pdf*, Oct 2025.

[11] D. Werber, A. Schwentner, and E. M. Biebl, "Investigation of RF transmission properties of human tissues," *Advances in Radio Science*, vol. 4, no. 4, pp. 357–360, sep 2006.

[12] H.-Z. T. Chen and A. S.-L. Lou, "A study of rf power attenuation in biotissues," *Journal of Medical and Biological Engineering*, vol. 24, no. 3, pp. 141–146, 2004.

[13] W. J. Tomlinson, S. Banou, C. Yu, M. Stojanovic, and K. R. Chowdhury, "Comprehensive survey of galvanic coupling and alternative intra-body communication technologies," *IEEE Communications Surveys & Tutorials*, vol. 21, no. 2, pp. 1145–1164, 2018.

[14] J. Park and P. P. Mercier, "Magnetic human body communication," in *2015 37th Annual International Conference of the IEEE Engineering in Medicine and Biology Society (EMBC)*. IEEE, 2015, pp. 1841–1844.

[15] S. Islam, R. K. Gulati, M. Domic, A. Pal, K. Kant, and A. Kim, "Performance evaluation of magnetic resonance coupling method for intra-body network (ibnet)," *IEEE Transactions on Biomedical Engineering*, vol. 69, no. 6, pp. 1901–1908, June 2022.

[16] R. K. Gulati, S. Islam, A. Pal, K. Kant, and A. Kim, "Characterization of magnetic communication through human body," *IEEE Consumer Communications and Networking Conference (CCNC)*, pp. 563–568, Jan 2022.

[17] H. Kia, R. Gulati, and K. Kant, "A study of magnetic resonance and ultrasound based through-the-body communications," *Proc. of IEEE WiMob conference*, Oct 2024.

[18] H. Kia and K. Kant, "Autotuning of resonant magnetic induction communications," *Accepted for DCOSS-IoT (Intl. conf. on dist. computing in Smart Systems and IoT), available at https://www.kkant.net/papers/qfactor_tuning.pdf*, April 2024.

[19] V. K. Sachan, S. A. Imam, and M. T. Beg, "Energy-efficient communication methods in wireless sensor networks: A critical review," *International Journal of Computer Applications*, vol. 39, no. 17, pp. 35–48, 2012.

[20] P. Pandit, H. Kia, and K. Kant, "Energy efficiency and communication accuracy tradeoff in intra-body networks," in *Proc. of ACM CHASE conf., Available at https://www.kkant.net/Pramita_CDMN_comm_paper.pdf*. New York, NY, USA: ACM, June 2025.

[21] CAP-XX, "Cap-xx gy series supercapacitor datasheet (v4.5)," February 2024. [Online]. Available: https://www.cap-xx.com/wp-content/uploads/2024/02/CAP-XX-GY-series-Datasheet-V4_5.pdf